Editors' Suggestion | Featured in Physics

Coherent Transfer of Spin Angular Momentum by Evanescent Spin Waves within Antiferromagnetic NiO

Maciej Dąbrowski,[1,*] Takafumi Nakano,[1,2] David M. Burn,[3] Andreas Frisk,[3] David G. Newman,[1] Christoph Klewe,[4] Qian Li,[5] Mengmeng Yang,[5] Padraic Shafer,[4] Elke Arenholz,[4] Thorsten Hesjedal,[6] Gerrit van der Laan,[3] Zi Q. Qiu,[5] and Robert J. Hicken[1,†]

[1]*Department of Physics and Astronomy, University of Exeter, Stocker Road, Exeter, Devon EX4 4QL, United Kingdom*
[2]*Spintronics Research Center, National Institute of Advanced Industrial Science and Technology (AIST), Tsukuba 305-8568, Japan*
[3]*Magnetic Spectroscopy Group, Diamond Light Source, Didcot OX11 0DE, United Kingdom*
[4]*Advanced Light Source, Lawrence Berkeley National Laboratory, Berkeley, California 94720, USA*
[5]*Department of Physics, University of California at Berkeley, California 94720, USA*
[6]*Department of Physics, Clarendon Laboratory, University of Oxford, OX1 Oxford 3PU, United Kingdom*

(Received 17 December 2019; accepted 6 April 2020; published 26 May 2020)

Insulating antiferromagnets have recently emerged as efficient and robust conductors of spin current. Element-specific and phase-resolved x-ray ferromagnetic resonance has been used to probe the injection and transmission of ac spin current through thin epitaxial NiO(001) layers. The spin current is found to be mediated by coherent evanescent spin waves of GHz frequency, rather than propagating magnons of THz frequency, paving the way towards coherent control of the phase and amplitude of spin currents within an antiferromagnetic insulator at room temperature.

DOI: 10.1103/PhysRevLett.124.217201

The need for energy efficient information technology has generated intense interest in media for processing data using new carriers including sound [1], light [2], and electron spin [3]. Recently, insulating antiferromagnets (AFMs) were shown to transport spin angular momentum via spin waves [4–8]. While robustness against magnetic perturbations and functionality at THz frequencies [9,10] are common to most AFMs, exceptionally long-distance spin transport [4] and current induced switching of the Néel vector by antidamping torques [11–13] have only been reported for insulating phases. Experiments have been restricted to dc spin currents, providing no insight into the underlying dynamic processes [14]. In particular, control of coherent spin currents, where the phase of a spin wave can be used to encode information [15], remains to be demonstrated.

It was predicted [16] that for a few nm thick AFMs with *biaxial* anisotropy, coherent excitation of evanescent spin waves can transfer angular momentum from the lattice to the spin system, resulting in amplification of the transmitted spin current. Although enhanced dc spin current transmission through thin (≤ 6 nm) NiO films has been detected by inverse spin Hall effect (ISHE) measurements [17–19], the microscopic mechanism is unclear, since alternative explanations based upon diffusion of thermal magnons can also reproduce the measured dependence of the dc spin current on NiO thickness [19,20]. To determine whether the spin angular momentum is transferred by coherent magnons [16,21,22] or via diffusion of thermal magnons [19,20], the coherence of the spin current must be verified. Measurements of ac spin current at nm length scales are crucial, but until now have not been reported.

In this Letter, we present experimental detection of coherent spin current propagation through epitaxial NiO (001) layers. Using element specific x-ray ferromagnetic resonance (XFMR) [23–26], the phase and amplitude of the magnetization precession within adjoining source and sink ferromagnetic (FM) layers are detected, so that the injection and transmission of pure ac spin current through NiO can be inferred. Two different scenarios are explored: (i) NiO directly coupled to the FM layers so that the propagation of spin current through both NiO interfaces is assisted by interfacial exchange coupling; and (ii) NiO decoupled from the sink layer by insertion of an additional nonmagnetic (NM) spacer layer so that propagation of the spin current through the NM is detected via the spin-transfer torque (STT) acting at the NM/FM interface.

The present study focuses on epitaxial NiO(001) within $Ni_{80}Fe_{20}(25)/Fe(1)/NiO(d)/Fe_{75}Co_{25}(5)$ structures (the FM layers are referred to as NiFe and FeCo) with NiO thickness $d = 4$, 6, 9 and 12 nm, grown on $MgO(5)/MgO(001)$ and capped with a MgO(3) layer (thicknesses in nm). Fe was grown on the NiO to ensure a smooth epitaxial interface. A series of samples with an additional 5 nm thick layer of Ag or Pd inserted between the $NiO(d)$ and FeCo layers was grown to suppress the interfacial exchange coupling between these layers. The samples were field cooled from 550 K to room temperature in a 1 T field applied along the FeCo[100]||NiO[110] axis. The quality and crystalline order of particular layers was

confirmed by low energy electron diffraction (LEED) (see the Supplemental Material [27]). Based on x-ray magnetic linear dichroism (XMLD) measurements with variable x-ray polarization direction, and x-ray magnetic circular dichroism (XMCD) hysteresis loops acquired in a transverse geometry, i.e., with the x-ray wave vector perpendicular to the applied field, it was found that the NiO moments lie in plane and at 90° to the moments in the adjacent FeCo and NiFe layers, as for Co/NiO(001) [31,32]. Details of the 90° coupling are provided within the Supplemental Material [27].

XFMR experiments were carried out on beam lines 4.0.2 of the Advanced Light Source (USA) and I10 at the Diamond Light Source (UK), by varying the time delay between a synchronized radio frequency (rf) magnetic field, which pumped the spin precession, and circularly polarized x-ray pulses, which probed the oscillatory magnetization component along the x-ray wave vector. The x rays were incident at 50° with respect to the sample normal. The sample was placed face down on a coplanar waveguide (CPW), with a countersunk hole of 500 μm diameter allowing the x-ray beam to access the surface of the sample, while the transmitted x rays excited optical luminescence in the MgO substrate, which was detected by a photodiode mounted behind the sample. An excitation frequency of 4 GHz was used for all measurements.

By tuning the x-ray energy to the absorption edge of interest, XFMR signals from the NiFe source (Ni L_3 edge) and the FeCo sink (Co L_3 edge) were measured separately. Figure 1(a) shows the sample stack and the geometry for spin transport within the NiO film. XMCD hysteresis loops for Co and Ni for samples with $d = 4$ and 12 nm, with the magnetic field applied in the sample plane perpendicular to the field cooling direction, are shown in Fig. 1(b). The split loops result from uniaxial anisotropy induced by field cooling. Both FM layers switch at the same field values and are always collinear, as a result of the 90° coupling at the NiO interfaces (see the Supplemental Material [27] for details).

Precession of the NiFe and FeCo moments was measured in directly coupled NiFe/Fe/NiO(d)/FeCo structures near the NiFe resonance. Both the amplitude and phase of precession were extracted by fitting each XFMR delay scan to a sine wave, as shown for $d = 4$ nm in Fig. 2(a). To quantify the amplitude of precession, the FMR precession cone angle was estimated from the ratio between the dynamic XFMR signal (I_{XFMR}) and the static XMCD signal (I_{XMCD}) using $\theta = \arctan(I_{\mathrm{XFMR}}/I_{\mathrm{XMCD}})$ [24,26]. For $d = 4$ and 12 nm [Figs. 2(b), 2(c)], both layers exhibit a FMR peak with resonance field $\mu_0 H_r = (6.1 \pm 0.5)$ and $\mu_0 H_r = (2.1 \pm 0.5)$ mT, respectively. The FeCo FMR mode is well separated from that of the NiFe [as verified by vector network analyzer (VNA)-FMR] and so the observed precession of the FeCo must be induced by the NiFe precession. Notably, both layers precess exactly in

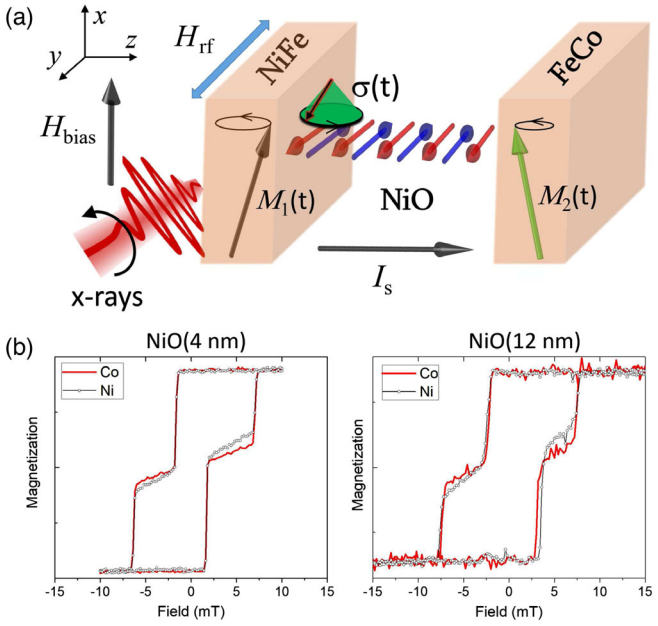

FIG. 1. (a) Schematic diagram of XFMR measurements of spin pumping in a FM/AFM/FM structure. Precession of the magnetization M_1 of the NiFe source layer about the bias field H_{bias} is induced by an in-plane rf magnetic field H_{rf}. The precession generates a spin current I_S with time-dependent spin polarization $\sigma(t)$ that has both dc (parallel to the x axis) and ac (confined within the yz plane) components [33,34]. The spin current propagates through the 90° coupled NiO layer and is absorbed at the NiO/FeCo interface, inducing precession of the FeCo magnetization M_2. By tuning the x-ray energy to the L_3 absorption edges of Ni and Co, the amplitude and phase of the precession, with respect to H_{rf}, can be detected independently for the NiFe and FeCo. (b) Element specific XMCD hysteresis loops for Co and Ni acquired with H_{bias} perpendicular to the field cooling direction (i.e., perpendicular to FeCo[100]||NiO[110]) for NiFe/Fe/NiO(4 nm)/FeCo and NiFe/Fe/NiO(12 nm)/FeCo samples.

phase, while the phase changes by 180° as the field is swept through the resonance [Fig. 2(d)]. The in-phase precession was observed for all NiO thicknesses studied. The precession induced in the FeCo layer results from *ac* spin current pumped by the NiFe precession and propagating through the NiO layer. In contrast to the NM/AFM/NM and FM/AFM/NM structures in which propagation of spin current has previously been studied, here AFM moments are coupled at both interfaces and interfacial exchange coupling contributes to the transfer of spin angular momentum. The ratio of the cone angles $\theta_{\mathrm{Co}}/\theta_{\mathrm{Ni}}$ of the sink and source layer precession at H_r provides a measure of the ac spin current I_{ac} propagating through the NiO. The ratio is maximum at $d = 6$ nm and decays exponentially for larger d values [Fig. 2(e)], similar to previous studies of dc spin current [17–19]. This nonmonotonic thickness dependence suggests that spin current plays a significant role, and argues against the action of a single precessional mode of

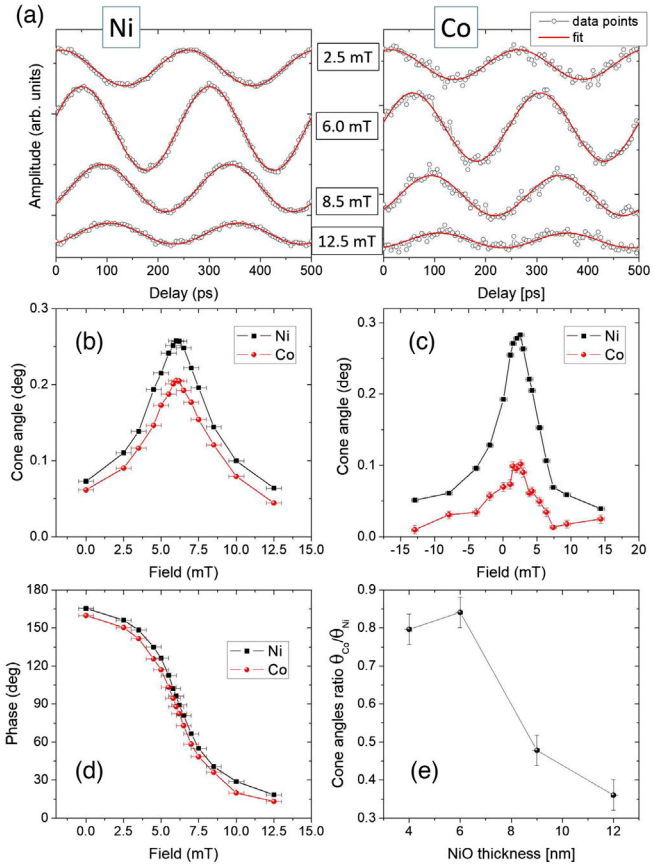

FIG. 2. (a) XFMR delay scans, with fitted sinusoids, that reveal precession of the Ni (NiFe layer) and Co (FeCo layer) moments at different bias fields for NiFe/Fe/NiO(4 nm)/FeCo. Amplitude of precession of the Ni and Co moments for (b) NiO (4 nm) and (c) NiO (12 nm). For samples with directly coupled layers, the FeCo and NiFe layers precess with the same phase, as shown in (d) for the sample with 4 nm thick NiO. (e) Ratio of the Co and Ni cone angles for different NiO thicknesses.

the exchange coupled layers, for which a monotonic thickness dependence would be expected.

To further demonstrate the propagation of ac spin current through NiO layers, experiments were performed on samples with a 5 nm thick NM layer of Ag or Pd inserted between the FeCo and NiO, to remove the interfacial exchange coupling between these layers. In Fig. 3, amplitudes (a),(c) and phases (b),(d) of the precession of FeCo and NiFe are shown for NiFe/Fe/NiO(2 nm)/Ag(5 nm)/FeCo [Figs. 3(a), 3(b)] and NiFe/Fe/NiO(4 nm)/Pd(5 nm)/FeCo [Figs. 3(c), 3(d)]. While the behavior of the NiFe is similar to that of the coupled layers shown in Fig. 2, both the amplitude and phase of the FeCo precession are very different upon insertion of the NM layer. The amplitudes are substantially reduced as the spin current must pass through an additional interface and 5 nm of NM material. The spin diffusion length in Pd is of order 2–10 nm [35] and comparable to the Pd layer thickness, while it is typically hundreds of nm in

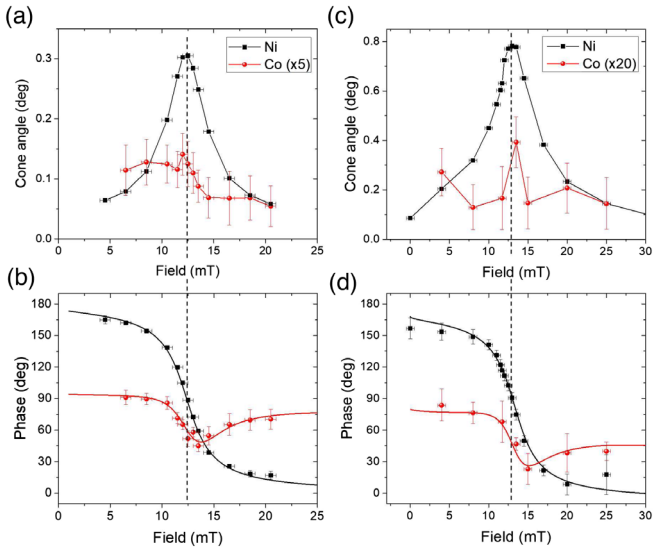

FIG. 3. (a),(c) Amplitude and (b),(d) phase of the magnetization precession for (a),(b) NiFe/Fe/NiO(2 nm)/**Ag(5 nm)**/FeCo and (c),(d) NiFe/Fe/NiO(4 nm)/**Pd(5 nm)**/FeCo. Dashed lines indicate the resonance fields $\mu_0 H_r = 12.5$ and 13.25 mT for the samples with Ag and Pd, respectively. In each case the phase variation in the FeCo layer shows a bipolar change at H_r and was fitted using Eq. (1).

Ag [36]. Also, the mechanism of transfer of spin angular momentum to the FM is different, and is assumed to result mainly from STT [23,24] rather than interfacial exchange coupling. Most importantly, the phase of the FeCo precession undergoes a bipolar phase variation as the field is swept through the NiFe resonance [Figs. 3(b), 3(d)], which results from the FeCo precession being driven by the total torque due to the rf field plus the ac spin current [23,24]. Although the bipolar phase variation can be clearly observed for all the measured samples with NM spacer layers, one cannot neglect interlayer exchange or dipolar coupling, which are still present in samples both with and without the 2 nm thick NiO, as can be deduced from magnetometry and XMCD hysteresis loops (see Fig. S3 in the Supplemental Material [27]). Both exchange and dipolar coupling lead to a unipolar rather than a bipolar variation of the phase [23,24,37]. To quantify the different contributions to the FeCo layer precession, the XFMR results can be modeled by a linearized macrospin solution of the Landau-Lifshitz-Gilbert equation that incorporates both interlayer coupling and the STT due to spin pumping [23,24,38]. The relative phase variation of the FeCo layer can be expressed by [14]

$$\tan(\phi_{\mathrm{FeCo}} - \phi^0_{\mathrm{FeCo}}) = \frac{\beta_{\mathrm{cp}} \sin^2\phi_{\mathrm{NiFe}} - \beta_{\mathrm{sc}} \sin\phi_{\mathrm{NiFe}} \cos\phi_{\mathrm{NiFe}}}{1 + \beta_{\mathrm{cp}} \sin\phi_{\mathrm{NiFe}} \cos\phi_{\mathrm{NiFe}} + \beta_{\mathrm{sc}} \sin^2\phi_{\mathrm{NiFe}}}, \quad (1)$$

where ϕ^0_{FeCo} is the phase of the FeCo precession driven by the rf field alone, ϕ_{NiFe} is the phase of the NiFe precession

and β_{cp} and β_{sc} are dimensionless parameters expressing the contributions of the interlayer coupling and the spin current, respectively [14]. The phase data were fitted with β_{cp} and β_{sc} as variable parameters, with damping constants $\alpha_{NiFe} = 0.003$, $\alpha_{FeCo} = 0.01$ ($\alpha_{FeCo} = 0.02$ for the sample with Pd spacer), which fall within the range of reported values [24,39,40]. The experimental data are well reproduced for other samples with different NiO thicknesses [see Figs. 3(b), 3(d) and Sec. S3 of the Supplemental Material [27]].

The dependence of the ac spin current on the NiO film thickness was explored next. In Fig. 4(a), XFMR delay scans for FeCo/Ag(5 nm)/NiO(d)/Fe/NiFe samples are shown at their resonance fields (maximum amplitudes). An oscillatory XFMR signal associated with precession is seen for all samples and is largest for $d = 2$ nm, suggesting an enhancement compared to the case without NiO. The spin transfer efficiency can be quantified via the ratio of cone angles, $I_{ac} = \theta_{Co}/\theta_{Ni}$, as in the case of directly coupled layers. To simplify comparison with previous experiments and theoretical models concerning dc spin current [17,20], values of I_{ac} are normalized to $I_{ac(0)}$, the value for the sample without NiO. The dependence of $I_{ac}/I_{ac(0)}$ on NiO thickness for samples with 5 nm Ag spacer layer is shown in Fig. 4(b). The ac spin current nearly doubles upon insertion of 2 nm of NiO and then decreases for larger thickness values. This dependence closely resembles the enhancement of the dc spin current measured by ISHE experiments [17–19].

The presented results confirm the propagation of ac spin current through an AFM layer at a temperature well below the Néel temperature $T_N = 520$ K (for bulk NiO), suggesting that the spin current is mediated by coherent excitations of the AFM of GHz frequency. Despite the frequency mismatch between the GHz spin current and the THz magnon spectrum of the AFM, spin angular momentum may be transported by means of GHz evanescent AFM spin waves [16] or AFM magnon pair propagation [21]. For a FM/AFM/FM structure, if the exchange interaction throughout the structure is very strong, all the magnetic moments should be locked together, causing the magnetizations of the two FM layers to rotate in unison when magnetic field is applied. However, if the exchange interaction is reduced, the AFM magnetic order will no longer be rigid and there should be a small but finite twist in the alignment of the magnetic moments through the thickness of the AFM layer as the magnetization of the source FM layer is rotated. When the precessional character of the motion is also taken into account, this twist is in fact synonymous with the evanescent AFM spin wave modes proposed by Khymyn *et al.* [16].

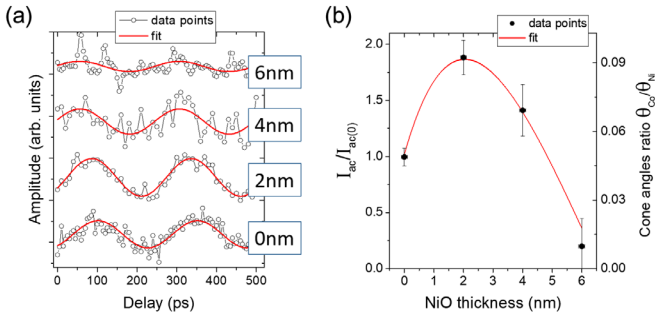

FIG. 4. (a) XFMR delay scans for the FeCo layer at H_r for samples with a 5 nm thick Ag spacer layer and NiO thickness $d = 0$, 2, 4, 6 nm. (b) Dependence on d of the spin current transmission efficiency $I_{ac}/I_{ac(0)}$ (the θ_{Co}/θ_{Ni} cone angle ratio). The solid line shows a fit to the model of Khymyn *et al.* [16].

Following Ref. [16] let us consider the spin current propagated through bulklike NiO by a pair of linearly-polarized evanescent AFM spin waves with eigenfrequencies $\omega_1 = 240$ GHz and $\omega_2 = 1.1$ THz that correspond to easy plane and out of plane magnon modes, respectively. Based on the observed static 90° interfacial coupling and XMLD measurements of the magnetic order of the NiO layers, it is assumed that (001) is the easy plane and [001] is the hard axis, so that both eigenmodes may be excited by coupling to the NiFe source layer. For 4 GHz excitation frequency, the ω_1 and ω_2 evanescent modes have penetration lengths of 22 and 5 nm, respectively [16]. Using Eq. (9) in Ref. [16], the best fit is obtained when the phase shift between the two spin waves $\psi = \pi/2 - 0.1$ [Fig. 4(b)]. The initial phase shift ψ at the NiFe/NiO interface is expected to be exactly $\pi/2$ in the present case since the precessing source layer has ac components within the yz plane [see Fig. 1(a)]. While the injected spin current can induce oscillations of the NiO spins in the z direction in the present geometry, the 90° exchange coupling allows oscillations to be induced in the x direction. Hence, the two linear evanescent modes with polarization along the x and z axes, with frequencies ω_1 and ω_2, respectively, are excited with a $\pi/2$ phase difference [Fig. 1(a)]. Therefore, the fit implies that these two evanescent wave modes differ in phase by about -0.1 rad after propagating through 6 nm of NiO and 5 nm of Ag. Although the dependence of the spin current upon NiO thickness for directly coupled layers [in Fig. 2(e)] is very similar to that obtained from the model of Khymyn *et al.* (see Fig. 2 in Ref. [16]), one should remember that the model describes a FM/AFM/NM trilayer and does not take into account the magnetic coupling at the interface between the AFM layer and the sink FM layer. Therefore the model is not directly applicable to the data within Fig. 2(e).

Other models have been proposed in which the GHz spin current is mediated by THz frequency magnons within an adiabatic approximation [14,22]. The observation of ac spin current places an upper limit of about 100 ps on the time required for a suitable THz magnon population to form. Specifically, it is necessary to explain both how THz magnons can be excited in an AFM by the GHz precession

of the magnetization in an adjacent FM, and also how such magnons interact within the AFM to form a well-defined statistical distribution on the timescales required. Finally, the present measurements were performed at room temperature, well below T_N for the NiO layers studied [42], so it seems unlikely that thermal THz magnons could lead to the significant excitation of the sink layer magnetization observed in the XFMR experiments. This was further verified by XFMR measurements at lower temperatures for the NiFe/Fe/NiO(4 nm)/FeCo sample, where no significant change in amplitude of the FeCo magnetization precession was observed down to 100 K.

The evanescent spin wave model does not explicitly take temperature dependence into account, in contrast to the thermal magnon model [20], which can naturally explain the enhancement of the spin current near the Néel temperature T_N [19,41,43,44]. However, the AFM magnon frequencies decrease as T_N is approached [45,46], which should result in an increase in the penetration of the evanescent spin waves and hence an increase of the spin current. Further studies of ac spin current in NiO in the vicinity of T_N are desirable, but the construction of the XFMR apparatus does not currently permit the sample to be heated above room temperature.

In summary, it has been demonstrated that ac spin current of GHz frequency can efficiently propagate through epitaxial NiO layers of different thickness at room temperature. The ac spin current is enhanced for NiO thicknesses less than 6 nm, both with and without a nonmagnetic spacer layer inserted into the stack, in a manner consistent with previously reported experimental measurements of dc spin current and theoretical studies. The results show that the propagation of spin current through NiO layers is mediated by evanescent antiferromagnetic spin wave modes of GHz frequency rather than THz frequency magnons.

The authors acknowledge the Engineering and Physical Sciences Research Council (EPSRC) under Grants No. EP/P021190/1, No. EP/P020151/1, and No. EP/P02047X/1. This work was supported by U.S. Department of Energy, Office of Science, Office of Basic Energy Sciences, Materials Sciences and Engineering Division under Contract No. DE-AC02-05-CH11231 (van der Waals heterostructures program, KCWF16). Beamtime awarded on I10 at the Diamond Light Source (SI17745-1, SI19116-1 and SI20760-1) is acknowledged. This research used resources of the Advanced Light Source, which is a DOE Office of Science User Facility under Contract No. DE-AC02-05CH11231. T. N. acknowledges JSPS Overseas Research Fellowships. D. G. N. acknowledges support via the EPSRC Centre for Doctoral Training in Metamaterials (Grant No. EP/L015331/1).

*m.k.dabrowski@exeter.ac.uk
†r.j.hicken@exeter.ac.uk

[1] M. V. Gustafsson, T. Aref, A. F. Kockum, M. K. Ekström, G. Johansson, and P. Delsing, Science **346**, 207 (2014).
[2] M. Hase, M. Katsuragawa, A. M. Constantinescu, and H. Petek, Nat. Photonics **6**, 243 (2012).
[3] A. Khitun, M. Bao, and K. L. Wang, J. Phys. D **43**, 264005 (2010).
[4] R. Lebrun, A. Ross, S. A. Bender, A. Qaiumzadeh, L. Baldrati, J. Cramer, A. Brataas, R. A. Duine, and M. Kläui, Nature (London) **561**, 222 (2018).
[5] O. Gomonay, V. Baltz, A. Brataas, and Y. Tserkovnyak, Nat. Phys. **14**, 213 (2018).
[6] D. Hou, Z. Qiu, and E. Saitoh, NPG Asia Mater. **11**, 35 (2019).
[7] T. Jungwirth, X. Marti, P. Wadley, and J. Wunderlich, Nat. Nanotechnol. **11**, 231 (2016).
[8] Z. Qiu, D. Hou, J. Barker, K. Yamamoto, O. Gomonay, and E. Saitoh, Nat. Mater. **17**, 577 (2018).
[9] T. Satoh, S.-J. Cho, R. Iida, T. Shimura, K. Kuroda, H. Ueda, Y. Ueda, B. A. Ivanov, F. Nori, and M. Fiebig, Phys. Rev. Lett. **105**, 077402 (2010).
[10] N. Kanda, T. Higuchi, H. Shimizu, K. Konishi, K. Yoshioka, and M. Kuwata-Gonokami, Nat. Commun. **2**, 362 (2011).
[11] X. Z. Chen, R. Zarzuela, J. Zhang, C. Song, X. F. Zhou, G. Y. Shi, F. Li, H. A. Zhou, W. J. Jiang, F. Pan *et al.*, Phys. Rev. Lett. **120**, 207204 (2018).
[12] I. Gray, T. Moriyama, N. Sivadas, G. M. Stiehl, J. T. Heron, R. Need, B. J. Kirby, D. H. Low, K. C. Nowack, D. G. Schlom *et al.*, Phys. Rev. X **9**, 041016 (2019).
[13] L. Baldrati, O. Gomonay, A. Ross, M. Filianina, R. Lebrun, R. Ramos, C. Leveille, F. Fuhrmann, T. R. Forrest, F. Maccherozzi *et al.*, Phys. Rev. Lett. **123**, 177201 (2019).
[14] Q. Li, M. Yang, C. Klewe, P. Shafer, A. T. N'Diaye, D. Hou, T. Y. Wang, N. Gao, E. Saitoh, C. Hwang *et al.*, Nat. Commun. **10**, 5265 (2019).
[15] A. V. Chumak, V. Vasyuchka, A. Serga, and B. Hillebrands, Nat. Phys. **11**, 453 (2015).
[16] R. Khymyn, I. Lisenkov, V. S. Tiberkevich, A. N. Slavin, and B. A. Ivanov, Phys. Rev. B **93**, 224421 (2016).
[17] H. Wang, C. Du, P. C. Hammel, and F. Yang, Phys. Rev. Lett. **113**, 097202 (2014).
[18] C. Hahn, G. de Loubens, V. V. Naletov, J. B. Youssef, O. Klein, and M. Viret, Europhys. Lett. **108**, 57005 (2014).
[19] W. Lin, K. Chen, S. Zhang, and C. L. Chien, Phys. Rev. Lett. **116**, 186601 (2016).
[20] S. M. Rezende, R. L. Rodríguez-Suárez, and A. Azevedo, Phys. Rev. B **93**, 054412 (2016).
[21] G. Tatara and C. O. Pauyac, Phys. Rev. B **99**, 180405(R) (2019).
[22] S. Takei, T. Moriyama, T. Ono, and Y. Tserkovnyak, Phys. Rev. B **92**, 020409(R) (2015).
[23] M. K. Marcham, L. R. Shelford, S. A. Cavill, P. S. Keatley, W. Yu, P. Shafer, A. Neudert, J. R. Childress, J. A. Katine, E. Arenholz *et al.*, Phys. Rev. B **87**, 180403(R) (2013).
[24] J. Li, L. R. Shelford, P. Shafer, A. Tan, J. X. Deng, P. S. Keatley, C. Hwang, E. Arenholz, G. van der Laan, R. J. Hicken *et al.*, Phys. Rev. Lett. **117**, 076602 (2016).
[25] D. A. Arena, E. Vescovo, C.-C. Kao, Y. Guan, and W. E. Bailey, Phys. Rev. B **74**, 064409 (2006).
[26] G. van der Laan, J. Electron Spectrosc. Relat. Phenom. **220**, 137 (2017).

[27] See Supplemental Material at http://link.aps.org/supplemental/10.1103/PhysRevLett.124.217201 for details of the interfacial exchange coupling, the interlayer coupling, fitting of the phase of the magnetization precession, and LEED images, which includes Refs. [28–30].
[28] N. C. Koon, Phys. Rev. Lett. **78**, 4865 (1997).
[29] R. Cheng, D. Xiao, and J.-G. Zhu, Phys. Rev. Lett. **121**, 207202 (2018).
[30] Y. Meng, J. Li, P.-A. Glans, C. A. Jenkins, E. Arenholz, A. Tan, J. Gibbons, J. S. Park, C. Hwang, H. W. Zhao *et al.*, Phys. Rev. B **85**, 014425 (2012).
[31] E. Arenholz, G. van der Laan, R. V. Chopdekar, and Y. Suzuki, Phys. Rev. Lett. **98**, 197201 (2007).
[32] G. van der Laan, N. D. Telling, A. Potenza, S. S. Dhesi, and E. Arenholz, Phys. Rev. B **83**, 064409 (2011).
[33] H. J. Jiao and G. E. W. Bauer, Phys. Rev. Lett. **110**, 217602 (2013).
[34] D. Wei, M. Obstbaum, M. Ribow, C. H. Back, and G. Woltersdorf, Nat. Commun. **5**, 3768 (2014).
[35] X. D. Tao, Z. Feng, B. F. Miao, L. Sun, B. You, D. Wu, J. Du, W. Zhang, and H. F. Ding, J. Appl. Phys. **115**, 17C504 (2014).
[36] T. Kimura and Y. Otani, Phys. Rev. Lett. **99**, 196604 (2007).
[37] A. A. Baker, A. I. Figueroa, C. J. Love, S. A. Cavill, T. Hesjedal, and G. van der Laan, Phys. Rev. Lett. **116**, 047201 (2016).
[38] B. Heinrich, Y. Tserkovnyak, G. Woltersdorf, A. Brataas, R. Urban, and G. E. W. Bauer, Phys. Rev. Lett. **90**, 187601 (2003).
[39] A. J. Lee, J. T. Brangham, Y. Cheng, S. P. White, W. T. Ruane, B. D. Esser, D. W. McComb, P. C. Hammel, and F. Yang, Nat. Commun. **8**, 234 (2017).
[40] H. Głowiński, F. Lisiecki, P. Kuświk, J. Dubowik, and F. Stobiecki, J. Alloys Compd. **785**, 891 (2019).
[41] Z. Qiu, J. Li, D. Hou, E. Arenholz, A. T. N'Diaye, A. Tan, K.-i. Uchida, K. Sato, S. Okamoto, Y. Tserkovnyak *et al.*, Nat. Commun. **7**, 12670 (2016).
[42] C. Boeglin, O. Ersen, M. Pilard, V. Speisser, and F. Kronast, Phys. Rev. B **80**, 035409 (2009).
[43] K. Chen, W. Lin, C. L. Chien, and S. Zhang, Phys. Rev. B **94**, 054413 (2016).
[44] D. Hou, Z. Qiu, J. Barker, K. Sato, K. Yamamoto, S. Velez, J. M. Gomez-Perez, L. E. Hueso, F. Casanova, and E. Saitoh, Phys. Rev. Lett. **118**, 147202 (2017).
[45] A. J. Sievers and M. Tinkham, Phys. Rev. **129**, 1566 (1963).
[46] T. Moriyama, K. Hayashi, K. Yamada, M. Shima, Y. Ohya, and T. Ono, Phys. Rev. Mater. **3**, 051402 (2019).